Organic Electronics 13 (2012) 1213–1222

Contents lists available at SciVerse ScienceDirect

Organic Electronics

journal homepage: www.elsevier.com/locate/orgel

Theoretical study on charge transport properties of cyanovinyl-substituted oligothiophenes

Yu-Ai Duan, Yun Geng, Hai-Bin Li, Xiao-Dan Tang, Jun-Ling Jin, Zhong-Min Su *

Institute of Functional Material Chemistry, Faculty of Chemistry, Northeast Normal University, Changchun 130024, China

ARTICLE INFO

Article history:
Received 29 December 2011
Received in revised form 14 March 2012
Accepted 17 March 2012
Available online 10 April 2012

Keywords:
Cyanovinyl
Oligothiophene
Intermolecular interaction
Anisotropy
Density function theory

ABSTRACT

When the oligothiophene is substituted by dicyanovinyl (DCV) or tricyanovinyl (TCV) group, how does its transport property change? Here, we will mainly focus on exploring the influence on charge transport properties of introducing a strong electron-withdrawing DCV/TCV group to the thiophene units within Marcus–Levich–Jortner formalism at the level of density functional theory. The results show that the introduction of cyanovinyl-substituents improves the molecular π-stacking, decreases the frontier molecular orbital energy levels and reorganization energies, and increases the transfer integrals and mobilities, comparing with their parent thiophene molecules. It is interesting to find the phenomenon that enriching intermolecular interactions can be favorable for controlling the transport channel and thus get high mobility, which would be shown by the angular resolution anisotropic mobilities analysis. Besides, the simulated packing motifs of dimers for **3a** and **3b** without crystal structures reported indicate that their packing may form the slip π–π stacking, and that **3b** may be a good ambipolar material. In a word, compared with corresponding thiophene analogues and tetracyanoquinodimethane, these compounds may become the candidates for the n-type or ambipolar organic semiconductor materials.

1. Introduction

During the past several years, the organic semiconductor materials have been extensively studied both in experiment and theory [1–6]. They are widely used in organic light-emitting diodes (OLED) [7,8], organic field effect transistors (OFET) [9–11] and organic photovoltaic cells (OPV) [12,13] because of their potential advantages such as mechanical flexibility, low cost, easy fabrication and so on. However, the development of organic n-type materials lags behind the p-type materials due to their instability at the air conditions and lower charge carrier mobility [14–16]. Therefore, the design and develop of high-performance and ambient-stable n-channel materials is crucial for the development of organic electronics.

In recent years, the approaches to achieve n-type materials with high mobilities and air stabilities have been reported by incorporating strong electron-withdrawing groups, such as –CN, –F, and –Cl and so on [17–19]. With these electronegative groups, their frontier energy levels can be effectively tuned and the molecular packing can be engineered. It has been proved that attaching electron-withdrawing groups on p-channel frameworks is an effective strategy to lower the lowest unoccupied molecular orbital (LUMO) levels and convert materials into n-channel organic semiconductors (OSCs) [20], such as the representative n-type material tetracyanoquinodimethane (**TCNQ**) [21]. Meanwhile, thiophene-based organic semiconductors have been extensively investigated in organic thin film transistor (OTFT) applications due to their excellent hole transport performance [22–27]. Recent works show that oligothiophene substituted by electron-withdrawing groups can serve as n-type transporting materials [18,28,29]. For instance, Bader et al. recently designed and

* Corresponding author. Tel.: +86 431 85099108; fax: +86 431 85684009.
E-mail address: zmsu@nenu.edu.cn (Z.-M. Su).

1566-1199/$ - see front matter © 2012 Elsevier B.V. All rights reserved.
http://dx.doi.org/10.1016/j.orgel.2012.03.026

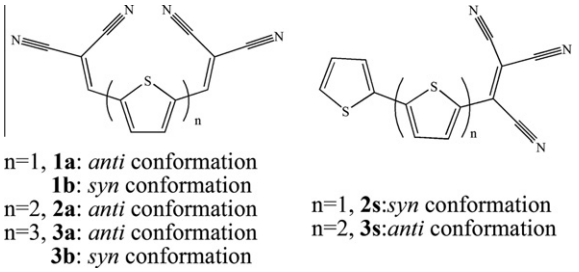

Fig. 1. Molecular models investigated in this work.

synthesized a new series of cyanovinyl-substituted oligothiophene derivatives: DCV- and TCV-substituted compounds (Fig. 1) [28,29], which are considered to be potential excellent optoelectronic materials and could be applied in organic electronics [30–33]. Especially, they own several favorable structural features, such as good planarity, π-stacked formation, strong intermolecular interactions, and easy of gaining and losing of the electron by introducing cyanovinyl to the thiophene. Therefore, they are expected to show ambipolar or electron transport properties [28,29].

In this study, we systematically investigated the influence of cyanovinyl introduced on geometric and electronic structures, ionization potentials and electronic affinities, reorganization energies, transfer integrals and mobilities of all the molecules shown in Fig. 1 using density functional theory (DFT) calculations. Moreover, in order to preliminarily evaluate the charge transport properties of **3a** and **3b** with no crystal structures, we simulated the molecular packing of **3a** and **3b** by dispersion-corrected DFT (DFT-D) method and calculated the hole and electron hopping rates based on Marcus–Levich–Jortner theory. Finally, the relationship of the angular resolution anisotropic mobility and the intermolecular interaction were discussed in detail in Section 3.5. The results suggest that introducing a strong electron-withdrawing cyanovinyl group to the thiophene units could result in improved carrier transport performance by enriching intermolecular interactions and transform the type of charge carrier. We hope these discussions can advance reasonable design of high-performance n-type materials.

2. Computational methods

The geometric structures of all systems (in Fig. 1) were optimized at PBE0/6-31 + G(d,p). Based on the optimized molecular geometries, vibrational frequencies were calculated by employing the same functional and basis set. The intramolecular reorganization energies were computed by two methods: (a) the normal-mode (NM) analysis, which was employed to provide the partition of the total geometry relaxation into the contributions from individual vibrational mode (provided in the supplementary); (b) the adiabatic potential-energy surfaces approach [34,35] at B_λLYP (%HF = 25.33)/6-31 + G(d,p) level, which has been proved to accurately estimate the internal reorganization energy [36–38]. Furthermore, dispersion-corrected density functional (B97-D) together with cc-pVDZ calculation was carried out to optimize the structures of model dimers for **3a** and **3b**, with the purpose of simulating their molecular packing in a preliminary way. All the calculations were performed in the Gaussian 09 software package [39].

At present, there are mainly two theoretical models to describe the charge transport mechanism in organic crystal semiconductors: band model and hopping model. In general, the hopping mechanism is employed to estimate the transport properties of organic materials due to their weak intermolecular interactions, which may result in stronger electron–phonon coupling and localization of carriers at high temperatures [40,41]. While, for the well ordered organic crystals at low temperatures, the transport behavior is more rationally described by band model. Here, all the compounds were investigated using the hopping model at 300 K; and the band model was also employed to gain comprehensive insight into the charge transport trend. In hopping regime, the charge-hopping process is generally portrayed as a self-exchange electron-transfer reaction between neighboring molecules. The hopping rate between two adjacent molecular sites i and j within the framework of Marcus–Levich–Jortner formulation is given as follows [42,43]:

$$K_{hopping} = t_{ij}^2 \times \sqrt{\frac{\pi}{\hbar^2 k_B T \lambda_{class}}} \sum_{n=0}^{\infty} \left[\exp(-S_{eff}) \frac{S_{eff}^n}{n!} \times \exp\left(-\frac{(\lambda_{class} + n\hbar\omega_{eff})^2}{4\lambda_{class} k_B T} \right) \right] \quad (1)$$

where T is the temperature and defined as 300 K, λ_{class} is the classical contribution to the reorganization energy (generally the outer sphere contribution). Here, we set a radix (0.007 eV) of λ_{class} for our systems, t_{ij} represents the charge transfer integral between molecular i and j; $\hbar$ is the Planck constant divided by 2π; k_B is the Boltzmann constant. In this formulation, the effective Huang–Rhys factor S_{eff} and effective frequency ω_{eff} are defined as: $\omega_{eff} = \sum_j S_j \omega_j / \sum_j S_j$, $S_{eff} = \lambda_{\mathrm{int}}/\hbar\omega_{eff}$, which treat only a few modes quantum mechanically by mode average to consider the effect of quantum behavior. In general, when $\hbar\omega \gg k_B T$, quantum mechanical correction (vibrational factors) must be treated and thus the Marcus–Levich–Jortner formulation should be adopted; when $\hbar\omega \ll k_B T$, it can be assumed that classical and the simpler Marcus-type expression can be employed [44].

The charge transfer integrals of all hopping pathways selected from crystal structures were obtained by the site-energy corrected method [45,46], which calculate the effective transfer integral from the spatial overlap integral S_{12}, transfer integral V_{12}, and site energies $\varepsilon_{1(2)}$:

$$V_{12}^{eff} = \frac{V_{12} - \frac{1}{2}(\varepsilon_1 + \varepsilon_2) S_{12}}{1 - S_{12}^2} \quad (2)$$

where, S_{12}, V_{12}, and $\varepsilon_{1(2)}$ can be obtained from $S_{12} = \langle \Psi_1 | \Psi_2 \rangle$, $V_{12} = \langle \Psi_1 | H | \Psi_2 \rangle$, and $\varepsilon_{1(2)} = \langle \Psi_{1(2)} | H | \Psi_{1(2)} \rangle$. Among them, H is the Hamiltonian of the dimer system; Ψ_1 and Ψ_2 are the highest occupied molecular orbitals (HOMOs) or the lowest unoccupied molecular orbitals (LUMOs) of two monomers. All calculations are performed using PW91PW91/6-31G(d,p) method, which has been

proven to give reliable estimation of transfer integral [47,48].

The drift mobility μ can be evaluated from the Einstein relation:

$$\mu = \frac{e}{k_B T} D \tag{3}$$

Here, e is the electronic charge, and D is the diffusion coefficient which can be approximately evaluated from the charge-transfer rate k as, $D = \lim_{t\to\infty} \frac{1}{2d} \frac{\langle x(t)^2 \rangle}{t} \approx \frac{1}{2d} \sum_i r_i^2 k_i P_i$, where d is the spatial dimension, k_i is the hopping rate along the specific hopping path i, r_i is the centroid distance between center molecule and neighbor i, and P_i is the relative probability for the charge carrier to a particular ith pathway, $P_i = k_i / \sum_i k_i$.

Meanwhile, to corroborate the reliability of the hopping model, the electronic band-structure calculations were also performed with VASP [49–51] using PBE exchange–correlation functional and a plane-wave basis set. The integrations over the Brillouin zone were sampled by $4 \times 4 \times 1$ k-points for **1b**, $7 \times 1 \times 3$ k-points for **2a**, $7 \times 2 \times 1$ k-points for **2a**·CH_2Cl_2, $3 \times 1 \times 4$ k-points for **2s**, $1 \times 7 \times 3$ k-points for **3s** and $5 \times 5 \times 2$ k-points for **TCNQ**, using the Monkhorst–Pack scheme [52].

3. Results and discussion

3.1. Geometric and electronic structures

Three functionals, B3LYP, BP86 and PBE0, were employed to optimize the geometry of **1b** to check the reliability of the theoretical level. The calculated results are collected in Table S1 in comparison with the available experimental values (crystal structures), and demonstrates that PBE0 give more reliable values than other two functionals. Thereby, the structures of all systems here were optimized at the PBE0/6-31 + G(d,p) level. The calculated results indicate that all these compounds are planar or nearly planar. For isomers **1a** and **1b**, the total energy difference of 0.002 eV between them suggests that they exist with stability. Besides, it is noted that the absolute values of total energy for all systems increase with the increasing of the repeating thiophene unit.

Table 1
The calculated adiabatic, vertical ionization potentials (IP (v) and IP (a)) and electronic affinities (EA (v) and EA (a)), for all compounds based on PBE0/6-31 + G(d,p) level (energies in eV).

Molecule	IP (v)	IP (a)	EA (v)	EA (a)
1a	8.95	8.86	3.00	3.17
1b	8.89	8.80	2.92	3.09
2a	8.12	8.03	2.86	3.01
3a	7.63	7.52	2.81	2.97
3b	7.59	7.49	2.79	2.94
2s	8.14	7.99	2.53	2.63
3s	7.51	7.37	2.64	2.72
TCNQ	9.16	9.08	3.64	3.78

Moreover, to simulate the influence of solid state packing environment, the geometries of **1b**, **2a**, **2s**, **3s** and **TCNQ** were also optimized by quantum mechanical/molecular mechanics (QM/MM) method. The force field for MM is the Universal Force Field (UFF). QM/MM could consider the influences of solid state environment. By comparing with the geometries optimized at single molecule scale, we found that all the geometries obtained from QM/MM are almost same as former. In addition, the frontier molecular orbital energies obtained from these two methods are summarized in Table S2. Apparently, the energy level of HOMOs/LUMOs did not show significant change from the gas phase to the solid state. So it is reasonable that we take all the calculations in the gas phase.

The frontier molecular orbitals of all compounds, **BT** and **TCNQ** shown in Fig. 2 suggest that both LUMOs and HOMOs spread over the whole molecule. This good delocalization is favorable for carrier transport. It is found that the introduction of cyanovinyl group decreases the HOMO and LUMO levels, and hence improves air stabilities and abilities of electron injection compared with their parent compound **BT**. While for series **1–3**, the frontier molecule orbital energy levels rise slowly with increasing the number of the thiophene rings. Moreover, compared with the compounds **2a**, **3a** and **3b** with DCV substituent on both sides of the thiophene cores, **2s** and **3s** with TCV substituent on only one side have slightly higher orbital energy levels. The values of HOMO energy level ranging from −7.67 to −6.39 eV are lower than those of polythiophenes and

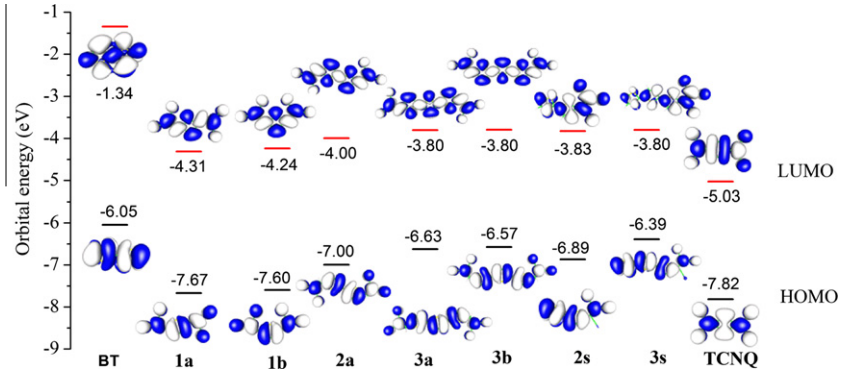

Fig. 2. Illustration of the frontier molecular orbitals for all compounds, bithiophene (**BT**) and **TCNQ** at PBE0/6–31 + G(d,p) level.

Table 2
Reorganization energies for all compounds calculated by B$_3$lyp/6-31 + G(d,p) based on adiabatic potential-energy surfaces approach (energies in eV).

	1a	1b	2a	3a	3b	2s	3s	TCNQ
λ_h	0.177	0.187	0.189	0.218	0.204	0.269	0.265	0.143
λ_e	0.356	0.361	0.262	0.328	0.314	0.198	0.174	0.287

pentacene (−4.9 eV), so the oxidative stabilities of these compounds in the environment are higher [53,54]. Their lower LUMO energy levels will facilitate the injection of electrons from metal electrode to organic layer in organic photoelectric devices, such as OLED. Meanwhile, the vertical and adiabatic ionization potentials (electronic affinities) for all systems were also calculated at PBE0/6-31 + G(d,p) level (Table 1). Recently, Chao and coworkers have reported that the threshold value of the adiabatic EA for air stability was 2.8 eV [55]. As can be seen from Table 1, the EA of DCV-substituted compounds are larger than 2.8 eV, and for TCV-substituted compounds, EA are found to be close to the threshold value. Therefore, all compounds are expected to be stable in the air environment. Combination of the orbital energy, the ionization potentials and electronic affinities, we predict that all compounds are the promising candidate for applications of the n-type materials. This finding would be further demonstrated in the following discussion.

3.2. Reorganization energy

Reorganization energy is one key parameter governing the carrier hopping rate. It includes the internal reorganization energy and the external reorganization energy. The former originate form contribution of intramolecular vibration and the latter is due to surrounding medium. Here, the intramolecular reorganization energies of all compounds were evaluated from adiabatic potential-energy surfaces approach based on B$_3$lyp (%HF = 25.33) /6-31 + G(d,p) level (Table 2). As seen in Table 2, the hole reorganization energies of the DCV-substituted thiophenes slightly increase with the increasing of the repeating thiophene unit, and for the TCV-substituted thiophenes, the hole reorganization energies are similar to each other. Overall, both of the hole and electron reorganization energies are relatively small, which indicates that all compounds could be a good carrier transport materials only from the standpoint of reorganization energy. Comparing the hole reorganization energies of these compounds with the ones of the typical hole transport materials **2T** (0.376 eV) and **3T** (0.425 eV) calculated at the same level, we find that introducing a strong electron-withdrawing cyanovinyl group lead to the reduction of reorganization energies, which is consistent with the finding of Sancho-García and Pérez-Jiménez. They found that the hole reorganization energies of cyanated tetracene derivatives decrease with the increasing of the number of cyano group [56].

Simultaneously, normal-mode (NM) analysis was employed to analyze the contributions of individual vibrational mode to the total intramolecular reorganization energies (Fig. S1). It is found that the main contributions of the reorganization energies for DCV-substituted thiophenes are derived from the stretching vibration of the C–C bond in the region of 1200–1500 cm^{-1}. While, the contributions of the stretching vibrations of the C–S bonds in the region of 500–750 cm^{-1} play an important role for hole reorganization energy of **2s**. For **3s**, torsion vibrations in the low frequency region of the entire molecular skeleton and the end of the thiophene unit make important contribution to hole and electron reorganization energies, respectively. Furthermore, it is clear from Table 2 and Fig. S1 that there is no significant difference in intramolecular reorganization energies calculated by these two methods, namely the normal mode analysis and adiabatic potential-energy surfaces approach. However, the reorganization energies calculated by the former is larger for **2s** and **3s** than that calculated by the latter, which could be ascribed to the breakdown of harmonic approximation, because the cyanovinyl on only one side of the thiophenes leads to the distortion of the end thiophene due to the imbalance of the two sides of molecule. In addition, the external (outer-sphere) reorganization energy, which is not easily estimated in crystal environment [57,58] and is usually much smaller in the solid phase than in liquids, also affect the chare transport performance of organic semiconductor. Herein, we have set a radix (0.007 eV) of the classical contributions to reorganization energy (λ_{class}) for our systems and estimated them using the same method as our previous work [16]. More importantly, McMahon and Troisi found that external reorganization energies is extremely small; for example, for the polyacene such as naphthalene, anthracene, tetracene and pentacene, their external reorganization energies are just from 0.001 to 0.007 eV [58].

3.3. Transfer integral

The transfer integral is another key parameter that plays an important role in determining the charge carrier mobility and its value mainly depends on both the relative positions of the interacting molecules and their frontier molecular orbital distributions, which have been confirmed by Brédas et al. [59,60]. Based on the crystal structures, the main carrier hopping pathways of **1b**, **2a**, **2a**·$\mathbf{CH_2Cl_2}$ (**2a** with dichloromethane solvent and the solvent molecules are not shown for clarity), **2s**, **3s** and **TCNQ** were selected and depicted in Fig. 3. The transfer integrals of all hopping pathways were calculated by the site-energy corrected method at PW91PW91/6-31G(d,p) level, and the results are listed in Table S3–S8, respectively.

As far as their intermolecular packing motifs were concerned, **1b** with DCV substituent at the 2, 5-position of the thiophene forms a slipped two-dimensional π-stacked arrangement, in which the cynao groups bring in C–N···H hydrogen-bond interactions between adjacent molecules. The results listed in Table S3 show that the largest hole and electron transfer integral of **1b** is 38.6 and 29.0 milli-electron volt (meV), respectively, which corresponds to the pathways with π–π intermolecular interaction. Meanwhile, the pathways with C–N···H hydrogen-bond interaction also have relative large transfer integrals, such as

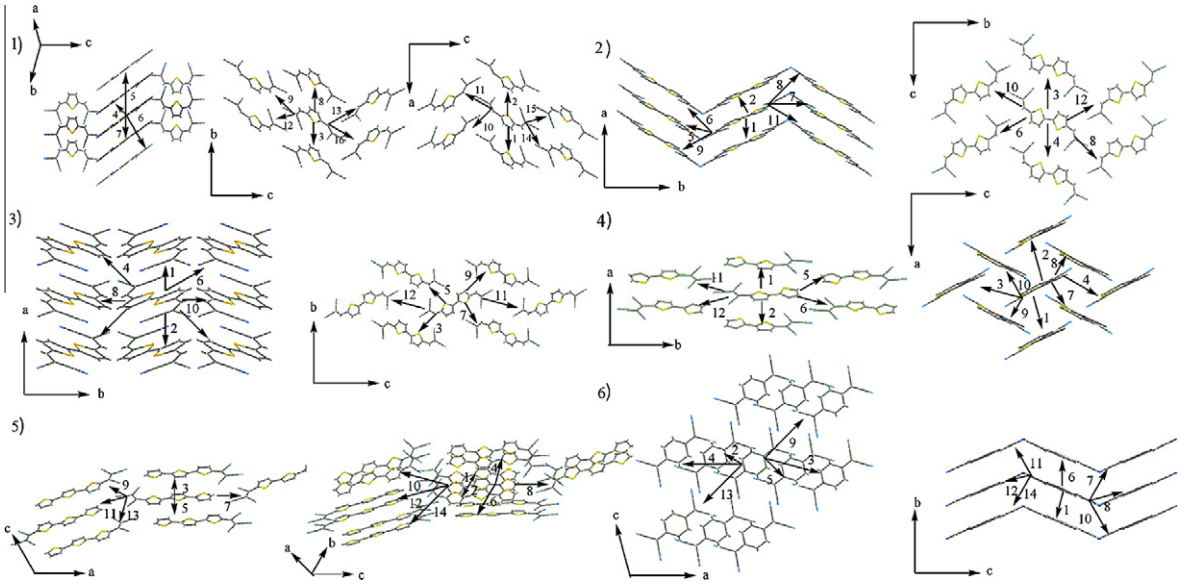

Fig. 3. Main charge-hopping pathways of (1) **1b**, (2) **2a**, (3) **2a**·CH_2Cl_2 (solvent molecules are not shown for clarity), (4) **2s**, (5) **3s** and (6) **TCNQ**.

pathways 11–13 and 15. Compared with **1b**, **2a** owns two thiophene units and forms an *anti*-structure, and its crystal shows the "herringbone" arrangement. It is well known that larger orbital overlaps between adjacent molecules would lead to larger transfer integrals generally. For **2a**, the pathway with the largest hole (68.5 meV) and electron (23.4 meV) transfer integral exhibits the face-to-face π–π packing, which is conducive to large intermolecular orbital overlap. Besides, strong C–N···H hydrogen-bond interactions also present in the crystal of **2a**. Because of the almost same hole and electron reorganization energies, the hole and electron mobilities of **2a** are considered to be larger than that of **1b**. While for **2a**·CH_2Cl_2, the crystal structure displays the slip-stacked π–π arrangement, and thus the maximum of transfer integrals for both hole (106.0 meV) and electron (49.7 meV) are larger than the solvent-free pseudo polymorph **2a**. For **2s**, TCV substitutes only locate on one side of the *syn*-bithiophene and lead to a "herringbone" arrangement with larger intermolecular distances, as compared with **2a**. The largest transfer integrals of **2s** are 22.3 meV for hole and 36.5 meV for electron, respectively. In **2s**, the primary intermolecular interactions are π–π interactions and the C–N···H hydrogen-bond interactions. **3s** with three thiophene units forms slip-stacked π–π arrangement with close intermolecular distance. The pathway 4 has the largest hole transfer integral (39.4 meV), while pathways 1 and 2 have the largest electron (50.6 meV) transfer integrals. In **3s**, both the C–N···S interactions and C–N···H hydrogen-bond interactions exist among neighboring molecules. For clarity, the main intermolecular interactions for **1b**, **2a**, **2a**·CH_2Cl_2, **2s** and **3s** are marked in Fig. 4, which will be discussed in detail in Section 3.5. As we all known, **TCNQ** is a typical electron transport materials and is a DCV-substituted system. In order to assess whether these compounds are suitable for electron transport materials or not, we compared their transfer integrals with those of **TCNQ**. The transfer integrals of all our compounds mentioned above are

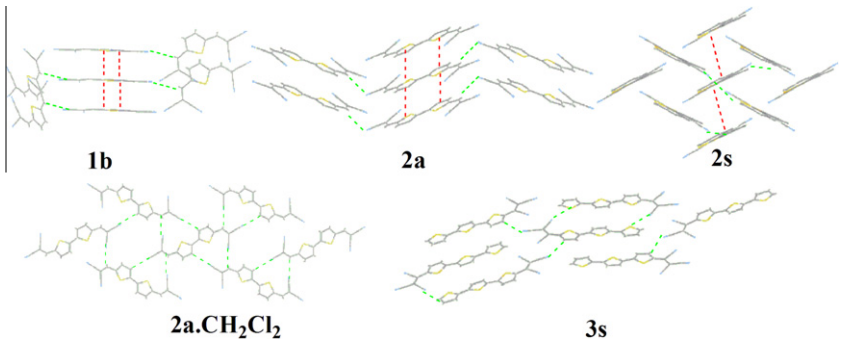

Fig. 4. Main intermolecular interactions for **1b**, **2a**, **2a**·CH_2Cl_2, **2s** and **3s**, the red represents π-π interaction and the green represents C–N···H hydrogen-bond interaction and C–N···S interaction.

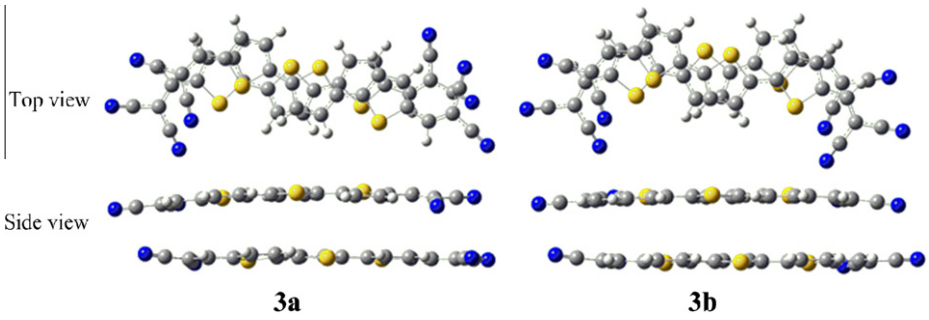

Fig. 5. Dimer models of **3a** and **3b**.

similar to or larger than **TCNQ** (28.4 meV for hole and 49.1 meV for electron). Combining the transfer integrals with the EA values, we speculate that most systems studied here may behave like **TCNQ** as the n-type materials.

As for **3a** and **3b** without crystal structure reported, the molecular packings with the face-to-face π stacked formation were simulated in a preliminary way at B97D/cc-pvdz level by setting 3.5 Å centroid distances, which has been often used to investigate the intermolecular packing. B97D functional has been recognized to provide more accurate estimate of intermolecular weak interaction [61,62]. In order to investigate the basis set effect, the geometric structure of **3a** was also optimized by three-zeta large basis set 6-311G(d) to minimize the basis set superposition error (BSSE) and to evaluate the effect of basis set size. And, interaction energies were calculated using counterpoise correction scheme taking BSSE into account [63]. In addition, we also compared the main hopping rate constant calculated by two basis sets. The results are summarized in Table S9, and show that there is no significant change for the BSSE-corrected interaction energies (ΔE), centroid distance (d) and the main hopping rate constants (k) calculated by cc-pVDZ and 6-311G(d). Thus, cc-pVDZ could be used to obtain these parameters mentioned above because of the compromise between the accuracy and computational efforts. The optimized structures at B97D/cc-pVDZ level are shown in Fig. 5. Due to the intermolecular interaction, the intermolecular relative orientations have some displacement from the initially set arrangement, namely face-to-face stacked formation. Based on the optimized structures, the hole and electron transfer integrals were calculated. The dimer centroid distances, hole and electron transfer integrals are listed in Table 3. We can find that the hole and electron transfer integrals are 68.6 and 56.7 meV for **3a**, and 36.9 and 94.8 meV for **3b**, respectively. As a result, we can infer reasonably that **3a** and **3b** possess high hole and electron mobilities and they may be potentials of excellent transport materials. It is important to point out that the hole and electron transfer integrals are rather large, although the slight overestimation of their values is possible using immature dispersion-corrected functional. Additionally, our investigation on the simulation of molecular packing of **3a** and **3b** is just tentative, because the accurate calculation of mobility needs to predict the crystal structure of organic semiconductor, which is still a great challenging task at current stage [64,65].

Table 3
Calculated hole and electron transfer integrals of **3a** and **3b** at PW91PW91/6-31G(d,p) level.

Molecule	Centroid distance (Å)	V_{Hole} (meV)	$V_{Electron}$ (meV)
3a	3.56	−68.6	−36.9
3b	3.53	56.7	−94.8

3.4. Drift mobility

In term of the parameters mentioned above, the hole (μ_h) and electron (μ_e) mobilities of the investigated compounds are estimated at room temperature (300 K). The results are summarized in Table 4. Apparently, the electron mobility of **TCNQ** calculated by Marcus–Levich–Jortner formulation is in well agreement with the experimental value, which has been reported to be 0.2–0.5 $cm^2/V\,s$ in the air [66]. From the results, we can find that (i) For DCV-substituted thiophenes, the hole mobilities are larger than electron mobilities; while for TCV-substituted thiophenes, the reverse happens, indicating that the number of cyanovinyl is a effective avenue to modulate the type of carrier. (ii) Both the hole and electron mobilities are increased with the increase of repeating thiophene unit. (iii) Both hole and electron mobility of **2a**·$\mathbf{CH_2Cl_2}$ is higher than that of **2a**, which is ascribed to less-ordered packing motifs and thus smaller transfer integrals of **2a**. (iv) The charge transfer rate constants of 1.56×10^{14} and $1.45 \times 10^{14}\ s^{-1}$ for hole, and 2.23×10^{13} and $2.33 \times 10^{14}\ s^{-1}$ for electron of **3a** and **3b** were obtained by Marcus–Levich–Jortner formulation, respectively (Table 4). Therefore, according to the carrier mobilities and hopping rate constants, **3b** and **2a**·$\mathbf{CH_2Cl_2}$ may be the good ambipolar materials, **2s** and **3s** are expected to show n-channel charge transport properties. In summary, we speculate that the DCV-substituted and TCV-substituted compounds may become the candidates of n-type or ambipolar semiconductors.

3.5. Anisotropy of mobility

The anisotropic mobility is an intrinsic property of charge transport in organic semiconductors [67,68]. In order to investigate the relationships among angular resolution anisotropic mobility, molecular structures, and packing, Han and coworkers proposed a theoretical model

Table 4
The effective frequencies ω_{eff} (eV), and effective Huang–Rhys factors S_{eff}, charge carrier mobilities μ ($cm^2/V\,s$) and the main hopping rate constants k (s^{-1}) for **1b**, **2a**, **2a·CH_2Cl_2**, **3a**, **3b**, **2s**, **3s** and **TCNQ** within Marcus–Levich–Jortner formulation.

	Hole				Electron			
	ω_{eff}	S_{eff}	μ_h	k_h	ω_{eff}	S_{eff}	μ_e	k_e
1b	0.134	1.40	1.32	6.89×10^{13}	0.169	2.14	0.351	1.85×10^{13}
2a	0.141	1.34	2.10	2.31×10^{14}	0.165	1.59	0.261	2.09×10^{13}
2a·CH_2Cl_2	0.142	1.32	5.15	5.59×10^{14}	0.161	2.10	0.521	5.67×10^{13}
3a	0.126	1.73		1.56×10^{14}	0.135	2.43		2.23×10^{13}
3b	0.143	1.42		1.45×10^{14}	0.159	1.98		2.33×10^{14}
2s	0.118	2.28	0.093	9.47×10^{12}	0.126	1.57	0.911	5.18×10^{13}
3s	0.116	2.29	0.692	2.93×10^{13}	0.116	1.50	3.38	1.06×10^{14}
TCNQ	0.182	0.79	1.13	6.86×10^{13}	0.104	2.76	0.489[a]	2.85×10^{13}

[a] The value in Ref. [63] is 0.2–0.5 $cm^2/V\,s$.

to simulate the anisotropic mobility [69,70]. Here, this model was also used to probe the relationship between the intermolecular interaction and the anisotropic mobility to gain insight into the influence of cyanovinyl groups. According to the projection of different hopping pathways to a transistor channel, we calculated the anisotropic hole and electron mobilities for each compounds, and the results were depicted in Fig. S2–S5 and Fig. 6. As seen from Fig. S2, both hole (0.2667 $cm^2/V\,s$) and electron (0.0201 $cm^2/V\,s$) mobilities of **1b** are isotropic, i.e., arbitrary selection of a transistor channel in *a*–*b* plane can obtain same carrier mobilities, which is just the thing to be aimed at for experimentalist. Combining with the discussion on transfer integrals and intermolecular interactions in Section 3.3, we can find that the π–π and C–N···H hydrogen-bond interaction play the same role in the charge carriers transport for **1b**. For **2a**, the hole and electron anisotropic mobilities in the *a*–*c* plane in Fig. 6 reveal that

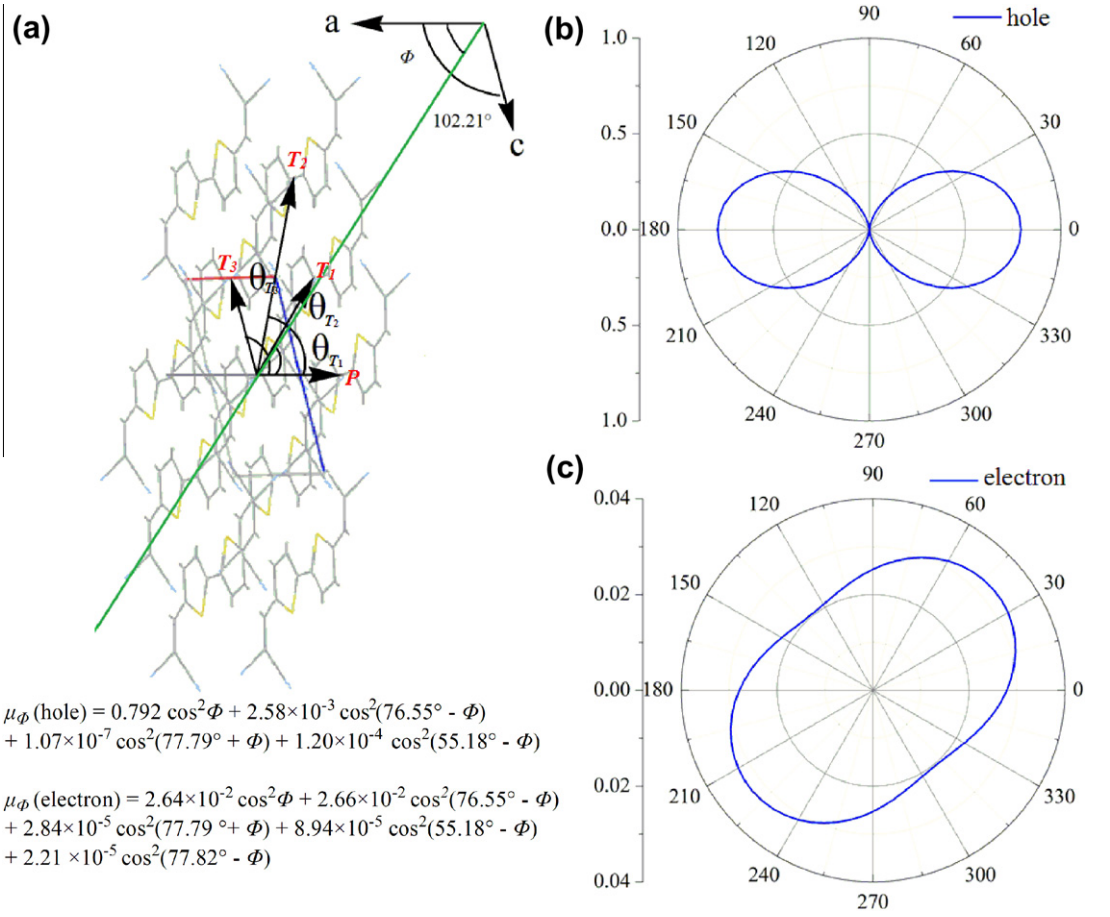

Fig. 6. (a) Illustration of projecting different hopping pathways to a transistor channel in the a–c plane of **2a** crystal; θ_P, θ_{T1}, θ_{T2} and θ_{T3} are the angles of *P*, T_1, T_2, and T_3 dimers relative to the reference crystallographic axis *a*; Φ is the angle of a transistor channel relative to the reference crystallographic axis *a*. (b) The simulated hole anisotropic mobilities and (c) electron anisotropic mobilities in the *a*–*c* plane of **2a**.

the highest hole mobilities (0.792 $cm^2/V\,s$) could be obtained when the transistor channels selected are along the 0° and 180° directions relative to the *a* axis, and these directions are found to correspond to the transport pathways with π–π intermolecular interactions. However, the highest electron mobility (0.0327 $cm^2/V\,s$) of **2a** occurs along the 39° and 219° directions relative to the *a* axis, which correspond to the projection of the four symmetrical pathways in the *a*–*c* plane with strong C–N···H hydrogen-bond interactions. These results show that intermolecular π–π interactions and C–N···H hydrogen-bond interactions play an important role and have a significant contributions to hole and electron charge transport, respectively. For **2a·CH_2Cl_2**, Fig. S3 illustrates that both the highest hole (1.944 $cm^2/V\,s$) and electron (0.0752 $cm^2/V\,s$) mobilities are along the parallel direction of *a* crystallographic axis, which correspond to the transport pathways 1 and 2 with π–π interactions. As for **2s**, Fig. S4(c) shows that the direction with the largest electron (0.354 $cm^2/V\,s$) mobility is along the *a* axis of the crystal cell However, the direction of its highest hole mobility (0.0255 $cm^2/V\,s$) (Fig. S4(b)) is perpendicular to the *a* axes in selected planes. The relevant pathway is pathways 1–4, which are all dominated by π–π interactions. The anisotropic hole and electron mobilities for **3s** are shown in Fig. S5. We can find that the 93° and 273° directions relative to the a axis of **3s** have the highest hole mobility (1.691 $cm^2/V\,s$). It is found that these directions correspond to the transport pathways with short C–N, C–C distances, which could provide effective orbital overlaps between neighboring slip-stacked molecules. However, the electron mobilities of **3s** are nearly isotropic, and the intermolecular π–π, C–N···S and C–N···H hydrogen-bond interaction in **3s** (vide supra) play the same role for the electron transporting. These calculated results show that the presence of the C–N···S, C–N···H hydrogen-bond and C–N short contacts introduced by cyanovinyl groups are favorable for the charge transport and provide another effective transport channels for charge carrier transport.

3.6. Band structure

To substantiate the reliability of the charge-transport hopping model, the electronic band structure along high symmetry directions are depicted in Fig. S6. In general, the appearance of both dispersive and flat bands is a reflection of anisotropy in the charge transport properties of the crystal; and the stronger dispersion of band is, the larger carrier mobility is. As seen from Fig. S6, the stronger dispersive valence band of **1b**, **2a** and **2a·CH_2Cl_2** implies that their hole mobilities are larger than electron mobilities. And for **2s**, **3s** and **TCNQ**, the dispersion magnitude of the valence band is smaller than that of conduction bands, indicating that their electron transport capacities are stronger than hole. These results are consistent with the results by means of the hopping model. Moreover, the purpose of our investigation is to gain insight into the relationship between structure and carrier transport property, not to calculate the accurate carrier mobility here. The hopping model is thus suitable.

4. Conclusions

The geometric and electronic structures, ionization potentials, electronic affinities, reorganization energies, transfer integrals and mobilities of the cyanovinyl-substituted thiophene derivatives were calculated and evaluated by DFT calculations and Marcus–Levich–Jortner formulation. According to these results, it is found that introducing a strong electron-withdrawing cyanovinyl group, whatever on one side or both sides of the thiophene units, the HOMOs and LUMOs of the investigated compounds are much lower than their parent thiophene molecules. The ionization potentials decrease with increasing of thiophene units; the electron affinities of all compounds are clearly in the range of air-stable n-type semiconductor materials. Combined with reorganization energies, transfer integrals and mobilities, we can speculate that DCV-substituted and TCV-substituted compounds may decrease the reorganization energy, promote π stacked arrangement, increase the transfer integral than the corresponding parent compounds. Moreover, DFT-D method was used to simulate the molecular packing of **3a** and **3b**, which have no crystal structures. Based on these optimized dimers, we tentatively estimated the charge transport properties of **3a** and **3b**, and inferred that **3b** may be the good ambipolar materials. From the above results, these compounds may achieve the materials from p-type to n-type or ambipolar transformation and the introduction of the cyanovinyl causes the C–N···H hydrogen-bond, C–N···S and C–N intermolecular interactions, which will be conducive to form the effective transporting network for the charge carriers. The studies on these compounds can provide some ideas for design and synthesize new organic semiconductors with high mobility by making full use of the various intermolecular interactions and make the n-type material rich and diverse.

Acknowledgements

The authors gratefully acknowledge financial support from NSFC (20903020 and 21131001), 973 Program (2009CB623605), SRF for ROCS. And we also thank the state key laboratory of theoretical and computational chemistry of Jilin University for supplying the VASP program.

Appendix A. Supplementary data

Supplementary data associated with this article can be found, in the online version, at http://dx.doi.org/10.1016/j.orgel.2012.03.026.

References

[1] G.H. Gelinck, T.C.T. Geuns, D.M. De Leeuw, High-performance all-polymer integrated circuits, Appl. Phys. Lett. 77 (2000) 1487–1489.
[2] A.P. Kulkarni, C.J. Tonzola, A. Babel, S.A. Jenekhe, Electron transport materials for organic light-emitting diodes, Chem. Mater. 16 (2004) 4556–4573.
[3] A.R. Murphy, J.M.J. Fréchet, Organic semiconducting oligomers for use in thin film transistors, Chem. Rev. 107 (2007) 1066–1096.

[4] Y. Shirota, H. Kageyama, Charge carrier transporting molecular materials and their applications in devices, Chem. Rev. 107 (2007) 953–1010.
[5] L. Wang, G. Nan, X. Yang, Q. Peng, Q. Li, Z. Shuai, Computational methods for design of organic materials with high charge mobility, Chem. Soc. Rev. 39 (2010) 423–434.
[6] Y. Geng, S.-X. Wu, H.-B. Li, X.-D. Tang, Y. Wu, Z.-M. Su, Y. Liao, A theoretical discussion on the relationships among molecular packings, intermolecular interactions, and electron transport properties for naphthalene tetracarboxylic diimide derivatives, J. Mater. Chem. 21 (2011) 15558–15566.
[7] C.W. Tang, S.A. Vanslyke, Organic electroluminescent diodes, Appl. Phys. Lett. 51 (1987) 913–915.
[8] J.H. Burroughes, D.D.C. Bradley, A.R. Brown, R.N. Marks, K. Mackay, R.H. Friend, P.L. Burns, A.B. Holmes, Light-emitting diodes based on conjugated polymers, Nature 347 (1990) 539–541.
[9] H.E. Katz, Organic molecular solids as thin film transistor semiconductors, J. Mater. Chem. 7 (1997) 369–376.
[10] H.E. Katz, A.J. Lovinger, J. Johnson, C. Kloc, T. Siegrist, W. Li, Y.Y. Lin, A. Dodabalapur, A soluble and air-stable organic semiconductor with high electron mobility, Nature 404 (2000) 478–481.
[11] M. Shim, A. Javey, N.W. Shi Kam, H. Dai, Polymer functionalization for air-stable n-type carbon nanotube field-effect transistors, J. Am. Chem. Soc. 123 (2001) 11512–11513.
[12] N.S. Sariciftci, L. Smilowitz, A.J. Heeger, F. Wudl, Photoinduced electron transfer from a conducting polymer to buckminsterfullerene, Science 258 (1992) 1474–1476.
[13] X. Zhan, Z.a. Tan, B. Domercq, Z. An, X. Zhang, S. Barlow, Y. Li, D. Zhu, B. Kippelen, S.R. Marder, A high-mobility electron-transport polymer with broad absorption and its use in field-effect transistors and all-polymer solar cells, J. Am. Chem. Soc. 129 (2007) 7246–7247.
[14] Q. Wu, R. Li, W. Hong, H. Li, X. Gao, D. Zhu, Dicyanomethylene-substituted fused tetrathienoquinoid for high-performance, ambient-stable, solution-processable n-channel organic thin-film transistors, Chem. Mater. (2011) 3138–3140.
[15] Z. Bao, Materials and fabrication needs for low-cost organic transistor circuits, Adv. Mater. 12 (2000) 227–230.
[16] Y. Geng, J. Wang, S. Wu, H. Li, F. Yu, G. Yang, H. Gao, Z. Su, Theoretical discussions on electron transport properties of perylene bisimide derivatives with different molecular packings and intermolecular interactions, J. Mater. Chem. 21 (2011) 134–143.
[17] C.-H. Li, C.-H. Huang, M.-Y. Kuo, Halogenated 6,13-bis(triisopropylsilylethynyl)-5,7,12,14-tetraazapentacene: applications for ambipolar air-stable organic field-effect transistors, Phys. Chem. Chem. Phys. 13 (2011) 11148–11155.
[18] X. Cai, M.W. Burand, C.R. Newman, D.A. da Silva Filho, T.M. Pappenfus, M.M. Bader, J.-L. Brédas, K.R. Mann, C.D. Frisbie, n- and p-channel transport behavior in thin film transistors based on tricyanovinyl-capped oligothiophenes, J. Phys. Chem. B 110 (2006) 14590–14597.
[19] M.-Y. Kuo, H.-Y. Chen, I. Chao, Cyanation: providing a three-in-one advantage for the design of n-type organic field-effect transistors, Chem. Eur. J. 13 (2007) 4750–4758.
[20] A. Facchetti, M. Mushrush, H.E. Katz, T.J. Marks, n-Type building blocks for organic electronics: a homologous family of fluorocarbon-substituted thiophene oligomers with high carrier mobility, Adv. Mater. 15 (2003) 33–38.
[21] A.R. Brown, D.M. de Leeuw, E.J. Lous, E.E. Havinga, Organic n-type field-effect transistor, Synth. Methods 66 (1994) 257–261.
[22] S. Mohapatra, B.T. Holmes, C.R. Newman, C.F. Prendergast, C.D. Frisbie, M.D. Ward, Organic thin-film transistors based on tolyl-substituted oligothiophenes, Adv. Funct. Mater. 14 (2004) 605–609.
[23] M. Halik, H. Klauk, U. Zschieschang, G. Schmid, S. Ponomarenko, S. Kirchmeyer, W. Weber, Relationship between molecular structure and electrical performance of oligothiophene organic thin film transistors, Adv. Mater. 15 (2003) 917–922.
[24] R.P. Ortiz, J. Casado, V. Hernández, J.T.L. Navarrete, J.A. Letizia, M.A. Ratner, A. Facchetti, T.J. Marks, Thiophene–diazine molecular semiconductors: synthesis, structural, electrochemical, optical, and electronic structural properties; implementation in organic field-effect transistors, Chem. Eur. J. 15 (2009) 5023–5039.
[25] J. Locklin, D. Li, S.C.B. Mannsfeld, E.-J. Borkent, H. Meng, R. Advincula, Z. Bao, Organic thin film transistors based on cyclohexyl-substituted organic semiconductors, Chem. Mater. 17 (2005) 3366–3374.
[26] C.R. Newman, C.D. Frisbie, D.A. da Silva Filho, J.-L. Brédas, P.C. Ewbank, K.R. Mann, Introduction to organic thin film transistors and design of n-channel organic semiconductors, Chem. Mater. 16 (2004) 4436–4451.
[27] X.-D. Tang, Y. Liao, H.-Z. Gao, Y. Geng, Z.-M. Su, Theoretical study of the bridging effect on the charge carrier transport properties of cyclooctatetrathiophene and its derivatives, J. Mater. Chem. 22 (2012) 6907–6918.
[28] M.M. Bader, P.-T.T. Pham, E.H. Elandaloussi, Dicyanovinyl-substituted oligothiophenes, Cryst. Growth Des. 10 (2010) 5027–5030.
[29] M.M. Bader, R. Custelcean, M.D. Ward, Tricyanovinyl-substituted oligothiophenes, Chem. Mater. 15 (2003) 616–618.
[30] C. Du, J. Chen, Y. Guo, K. Lu, S. Ye, J. Zheng, Y. Liu, Z. Shuai, G. Yu, Dicyanovinyl heterotetracenes: synthesis, solid-state structures, and photophysical properties, J. Org. Chem. 74 (2009) 7322–7327.
[31] M.M.M. Raposo, A.M.R.C. Sousa, G. Kirsch, P. Cardoso, M. Belsley, E. de Matos Gomes, A.M.C. Fonseca, Synthesis and characterization of dicyanovinyl-substituted thienylpyrroles as new nonlinear optical chromophores, Org. Lett. 8 (2006) 3681–3684.
[32] Y.-C. Shu, Z.-H. Gong, C.-F. Shu, E.M. Breitung, R.J. McMahon, G.-H. Lee, A.K.Y. Jen, Synthesis and characterization of nonlinear optical chromophores with conformationally locked polyenes possessing enhanced thermal stability, Chem. Mater. 11 (1999) 1628–1632.
[33] J.-M. Raimundo, P. Blanchard, N. Gallego-Planas, N. Mercier, I. Ledoux-Rak, R. Hierle, J. Roncali, Design and synthesis of push–pull chromophores for second-order nonlinear optics derived from rigidified thiophene-based π-conjugating spacers, J. Org. Chem. 67 (2001) 205–218.
[34] F. Yu, X. Tang, G. Yang, Y. Duan, Z. Su, A theoretical study of ambipolar organic transport material: 1,4-bis(pentafluorobenzyl)[60]-fullerene, Chem. Phys. Lett. 506 (2011) 255–259.
[35] G. Yang, Y. Si, Y. Geng, F. Yu, Q. Wu, Z. Su, Charge transport and electronic properties of n-heteroquinones: quadruple weak hydrogen bonds and strong π–π stacking interactions, Theor. Chem. Acc. 128 (2011) 257–264.
[36] J.C. Sancho-García, Assessment of density-functional models for organic molecular semiconductors: the role of Hartree-Fock exchange in charge-transfer processes, Chem. Phys. 331 (2007) 321–331.
[37] J.C. Sancho-García, A.J. Pérez-Jiménez, Accurate calculation of transport properties for organic molecular semiconductors with spin-component scaled MP2 and modern density functional theory methods, J. Chem. Phys. 129 (2008) 024103.
[38] J.C. Sancho-García, A.J. Pérez-Jiménez, Dependence of charge-transport parameters on static correlation self-interaction energy: the case of a 1,4-bis(phenylethynyl)benzene derivative conjugated molecule, J. Phys. Chem. A 112 (2008) 10325–10332.
[39] G.W.T.M.J. Frisch, H.B. Schlegel, G.E. Scuseria, J.R.C.M.A. Robb, G. Scalmani, V. Barone, B. Mennucci, H.N.G.A. Petersson, M. Caricato, X. Li, H.P. Hratchian, J.B.A.F. Izmaylov, G. Zheng, J.L. Sonnenberg, M. Hada, K.T.M. Ehara, R. Fukuda, J. Hasegawa, M. Ishida, T. Nakajima, O.K.Y. Honda, H. Nakai, T. Vreven, J.A. Montgomery Jr, F.O.J.E. Peralta, M. Bearpark, J.J. Heyd, E. Brothers, V.N.S.K.N. Kudin, R. Kobayashi, J. Normand, A.R.K. Raghavachari, J.C. Burant, S.S. Iyengar, J. Tomasi, N.R.M. Cossi, J.M. Millam, M. Klene, J.E. Knox, J.B. Cross, C.A.V. Bakken, J. Jaramillo, R. Gomperts, R.E. Stratmann, A.J.A.O. Yazyev, R. Cammi, C. Pomelli, J.W. Ochterski, K.M.R.L. Martin, V.G. Zakrzewski, G.A. Voth, J.J.D.P. Salvador, S. Dapprich, A.D. Daniels, J.B.F.O. Farkas, J.V. Ortiz, J. Cioslowski, a.D.J. Fox., Gaussian 09, Revision A.02, Gaussian Inc., Wallingford, CT, 2009.
[40] V. Coropceanu, J. Cornil, D.A. da Silva Filho, Y. Olivier, R. Silbey, J.-L. Brédas, Charge transport in organic semiconductors, Chem. Rev. 107 (2007) 926–952.
[41] X. Yang, L. Wang, C. Wang, W. Long, Z. Shuai, Influences of crystal structures and molecular sizes on the charge mobility of organic semiconductors: oligothiophenes, Chem. Mater. 20 (2008) 3205–3211.
[42] J. Jortner, Temperature dependent activation energy for electron transfer between biological molecules, J. Chem. Phys. 64 (1976) 4860–4867.
[43] R.A. Marcus, On the theory of oxidation-reduction reactions involving electron transfer. I, J. Chem. Phys. 24 (1956) 966–978.
[44] P.F. Barbara, T.J. Meyer, M.A. Ratner, Contemporary issues in electron transfer research, J. Phys. Chem. 100 (1996) 13148–13168.
[45] Y. Geng, H. Li, S. Wu, Y. Duan, Z. Su, Y. Liao, The influence of thienyl-S, S-dioxidation on the photoluminescence and charge transport properties of dithienothiophenes: a theoretical study, Theor. Chem. Acc. 129 (2011) 247–255.
[46] E.F. Valeev, V. Coropceanu, D.A. da Silva Filho, S. Salman, J.-L. Brédas, Effect of electronic polarization on charge-transport parameters in

molecular organic semiconductors, J. Am. Chem. Soc. 128 (2006) 9882–9886.
[47] M.C.R. Delgado, E.-G. Kim, D.t.A.d.S. Filho, J.-L. Bredas, Tuning the charge-transport parameters of perylene diimide single crystals via end and/or core functionalization: a density functional theory investigation, J. Am. Chem. Soc. 132 (2010) 3375–3387.
[48] X. Yang, Q. Li, Z. Shuai, Theoretical modelling of carrier transports in molecular semiconductors: molecular design of triphenylamine dimer systems, Nanotechnology 18 (2007) 424029.
[49] G. Kresse, J. Furthmüller, Efficient iterative schemes for ab initio total-energy calculations using a plane-wave basis set, Phys. Rev. B 54 (1996) 11169–11186.
[50] G. Kresse, J. Hafner, Ab initio molecular dynamics for liquid metals, Phys. Rev. B 47 (1993) 558–561.
[51] G. Kresse, J. Hafner, Ab initio molecular-dynamics simulation of the liquid-metal–amorphous-semiconductor transition in germanium, Phys. Rev. B 49 (1994) 14251–14269.
[52] J.D. Pack, H.J. Monkhorst, "Special points for Brillouin-zone integrations"—a reply, Phys. Rev. B 16 (1977) 1748–1749.
[53] K. Xiao, Y. Liu, T. Qi, W. Zhang, F. Wang, J. Gao, W. Qiu, Y. Ma, G. Cui, S. Chen, X. Zhan, G. Yu, J. Qin, W. Hu, D. Zhu, A highly π-stacked organic semiconductor for field-effect transistors based on linearly condensed pentathienoacene, J. Am. Chem. Soc. 127 (2005) 13281–13286.
[54] D.M. Nanditha, M. Dissanayake, R.A. Hatton, R.J. Curry, S.R.P. Silva, Operation of a reversed pentacene-fullerene discrete heterojunction photovoltaic device, Appl. Phys. Lett. 90 (2007) 113505.
[55] Y.-C. Chang, M.-Y. Kuo, C.-P. Chen, H.-F. Lu, I. Chao, On the air stability of n-channel organic field-effect transistors: a theoretical study of adiabatic electron affinities of organic semiconductors, J. Phys. Chem. C 114 (2010) 11595–11601.
[56] J.C. Sancho-García, A.J. Pérez-Jiménez, A theoretical study of π-stacking tetracene derivatives as promising organic molecular semiconductors, Chem. Phys. Lett. 499 (2010) 146–151.
[57] S. Di Motta, E. Di Donato, F. Negri, G. Orlandi, D. Fazzi, C. Castiglioni, Resistive molecular memories: influence of molecular parameters on the electrical bistability, J. Am. Chem. Soc. 131 (2009) 6591–6598.
[58] D.P. McMahon, A. Troisi, Evaluation of the external reorganization energy of polyacenes, J. Phys. Chem. Lett. 1 (2010) 941–946.
[59] J.L. Brédas, J.P. Calbert, D.A. Da Silva Filho, J. Cornil, Organic semiconductors: a theoretical characterization of the basic parameters governing charge transport, Proc. Natl. Acad. Sci. USA 99 (2002) 5804–5809.
[60] J.-L. Brédas, D. Beljonne, V. Coropceanu, J. Cornil, Charge-transfer and energy-transfer processes in π-conjugated oligomers and polymers: a molecular picture, Chem. Rev. 104 (2004) 4971–5004.
[61] S. Grimme, Semiempirical GGA-type density functional constructed with a long-range dispersion correction, J. Comput. Chem. 27 (2006) 1787–1799.
[62] R. Peverati, K.K. Baldridge, Implementation and performance of DFT-D with respect to basis set and functional for study of dispersion interactions in nanoscale aromatic hydrocarbons, J. Chem. Theory Comput. 4 (2008) 2030–2048.
[63] S. Simon, M. Duran, J.J. Dannenberg, How does basis set superposition error change the potential surfaces for hydrogen-bonded dimers?, J Chem. Phys. 105 (1996) 11024–11031.
[64] G.M. Day, T.G. Cooper, A.J. Cruz-Cabeza, K.E. Hejczyk, H.L. Ammon, S.X.M. Boerrigter, J.S. Tan, R.G. Della Valle, E. Venuti, J. Jose, S.R. Gadre, G.R. Desiraju, T.S. Thakur, B.P. van Eijck, J.C. Facelli, V.E. Bazterra, M.B. Ferraro, D.W.M. Hofmann, M.A. Neumann, F.J.J. Leusen, J. Kendrick, S.L. Price, A.J. Misquitta, P.G. Karamertzanis, G.W.A. Welch, H.A. Scheraga, Y.A. Arnautova, M.U. Schmidt, J. van de Streek, A.K. Wolf, B. Schweizer, Significant progress in predicting the crystal structures of small organic molecules – a report on the fourth blind test, Acta Crystallogr. Sect. B 65 (2009) 107–125.
[65] S.L. Price, Computed crystal energy landscapes for understanding and predicting organic crystal structures and polymorphism, Acc. Chem. Res. 42 (2009) 117–126.
[66] M. Yamagishi, Y. Tominari, T. Uemura, J. Takeya, Air-stable n-channel single-crystal transistors with negligible threshold gate voltage, Appl. Phys. Lett. 94 (2009) 053305.
[67] V.C. Sundar, J. Zaumseil, V. Podzorov, E. Menard, R.L. Willett, T. Someya, M.E. Gershenson, J.A. Rogers, Elastomeric transistor stamps: reversible probing of charge transport in organic crystals, Science 303 (2004) 1644–1646.
[68] C. Reese, Z. Bao, Organic single-crystal field-effect transistors, Mater. Today 10 (2007) 20–27.
[69] S.-H. Wen, A. Li, J. Song, W.-Q. Deng, K.-L. Han, W.A. Goddard, First-principles investigation of anistropic hole mobilities in organic semiconductors, J. Phys. Chem. B 113 (2009) 8813–8819.
[70] S. Wen, W.-Q. Deng, K.-L. Han, Ultra-low resistance at TTF–TCNQ organic interfaces, Chem. Commun. 46 (2010) 5133–5135.